Chyhareva, A., Gorodetskaya, I., Krakovska, S., Pishniak, D. & Rowe, P. (2021). Precipitation phase transition in austral summer over the Antarctic Peninsula.
*Ukrainian Antarctic Journal*, 1, 32—46.
https://doi.org/10.33275/1727-7485.1.2021.664



**A. Chyhareva [1, 2, *], I. Gorodetskaya [3], S. Krakovska [1, 2, *], D. Pishniak [2], P. Rowe [4]**

[1] Ukrainian Hydrometeorological Institute, State Service of Emergencies of Ukraine and National Academy of Sciences of Ukraine, Kyiv, 03028, Ukraine
[2] State Institution National Antarctic Scientific Center, Ministry of Education and Science of Ukraine, Kyiv, 01601, Ukraine
[3] Centre for Environmental and Marine Studies, Department of Physics, University of Aveiro, Aveiro, 3810-193, Portugal
[4] NorthWest Research Associates, Redmond, Washington, 98052, USA

*** Corresponding authors:** chyhareva@ukr.net, SvitlanaKrakovska@gmail.com

# Precipitation phase transition in austral summer over the Antarctic Peninsula

**Abstract.** Investigating precipitation phase transitions is crucial for improving our understanding of precipitation formation processes and impacts, particularly in Polar Regions. This study uses observational data and numerical modelling to investigate precipitation phase transitions in the western and northern Antarctic Peninsula (AP) during austral summer. The analysis is based on the ERA5 reanalysis product, dynamically downscaled using the Polar-WRF (Polar Weather Research and Forecasting) model, evaluated using regular meteorological observations and additional measurements made during the Year of Polar Prediction special observing period. We analyse three cases of extra-tropical cyclones bringing precipitation with phase transitions, observed at the Chilean station Professor Julio Escudero (King George Island, north of the AP) and the Ukrainian Antarctic Akademik Vernadsky station (western side of the AP) during the first week of December 2018. We use observed and modelled near-surface air temperature and pressure, precipitation amount and type, and vertical temperature profiles. Our results show that precipitation type (snow or rain) is well-represented by ERA5 and Polar-WRF, but both overestimate the total amount of precipitation. The ERA5 daily variability and vertical air temperature profile are close to the observed, while Polar-WRF underestimates temperature in the lower troposphere. However, ERA5 underestimates the temperature inversion, which is present during the atmospheric river event, while Polar-WRF represents that inversion well. The average weekly temperature, simulated with Polar-WRF, is lower compared to ERA5. The Polar-WRF fraction of snow in the total precipitation amount is higher than for ERA5; nevertheless, Polar-WRF represents the precipitation phase transition better than ERA5 during the event, associated with an atmospheric river. These case studies demonstrated a relationship between specific synoptic conditions and precipitation phase transitions at the AP, evaluated the ability of the state-of-the-art reanalysis and regional climate model to represent these events, and demonstrated the added value of combined analysis of observations from the western and northern AP, particularly for characterizing precipitation during synoptic events affecting the entire AP.

**Keywords:** Antarctic Peninsula, Ukrainian Antarctic Akademik Vernadsky station, Chilean station Professor Julio Escudero, precipitation phase, ERA5, Polar-WRF, air temperature, atmospheric pressure

## 1 Introduction

Regional manifestations of global climate warming are exceptionally strong in the Polar Regions. The Antarctic Peninsula (AP), in particular, has experienced the highest warming rate over Antarctica during recent decades. For example, there is a statistically significant warming trend, $0.49 \pm 0.28$ °C decade$^{-1}$ in 1957—2016 at the Faraday/Akademik Vernadsky station (Jones et al., 2019). Among the consequences of climate change

that can have critical impacts both regionally and globally is changing precipitation. Precipitation on the AP is controlled by synoptic-scale atmospheric circulation, which transports moisture from lower latitudes (Turner et al., 1995; Krakovskaia & Pirnach, 2003; Gonzalez et al., 2018). Precipitation is a major positive component of the Antarctic total mass balance, controlling its interannual variability (The IMBIE team, 2018; Rignot et al., 2019).

A recent study by Vignon et al. (2021) showed that a significant portion of the annual precipitation on the western AP occurs as rainfall. The chances of rain and associated surface melt in West Antarctica and the AP increase markedly during warm air intrusions and atmospheric rivers (Wille et al., 2019; Nicolas et al., 2017). Recent studies of precipitation projections show increases in consecutive wet days (Chyhareva et al., 2019) and rain and melt days (Bozkurt et al., 2021; Vignon et al., 2021) in the AP region during the 21st century, indirectly indicating that surface melt will continue.

Polar clouds and precipitation impact the radiative balance over the AP directly by influencing both shortwave and longwave radiative fluxes and indirectly by modulating the spectral dependence of the albedo. At the same time, our understanding of the microphysical properties of clouds and precipitation in Antarctica, particularly their association with Precipitation Phase Transitions (PPT), suffers from a scarcity of observations (Lachlan-Cope et al., 2016). One of the first applications of spectral cloud models in the AP region to the study of microphysical properties of cloud and precipitation revealed that in thermodynamic conditions of a deep extra-tropical cyclone, the liquid precipitation phase was less dependent on the concentration of cloud condensation nuclei than solid phase on ice nuclei (Krakovskaia & Pirnach, 2000). Correct representation of cloud and precipitation formation processes and precipitation type in polar numerical models remains a significant challenge (Kay et al., 2016; Listowski & Lachlan-Cope, 2017).

Climate models also have difficulties in representing snowfall amounts in Antarctica (Agosta et al., 2015). These errors are likely due to the challenge of representing cloud and precipitation microphysics, particularly precipitation phase and PPT in global and regional climate models, which typically rely on simplified parameterizations. For example, in the simplest parameterizations, it is common to assume that the phase of precipitation is determined by temperature alone, namely that it is raining at temperatures above 0 °C and snowing below 0 °C. However, the water freezing point depends on the presence and characteristics of aerosols and pure liquid droplets can exist down to –40 °C; snowflakes can exist in a warm layer, depending on the fall speed (Yuter et al., 2006). Snow and rain have very different properties and, consequently, different effects on land albedo, mass balance, hydrology, and climate (Dai, 2008).

In polar regions, uncertainties in weather forecasting are higher than for middle latitudes because of the lack of observational data for model evaluation and data assimilation. In recent decades, significant progress has been achieved both in increasing cloud and precipitation observations and improving polar cloud parameterizations (Bromwich et al., 2012). Further, new state-of-the-art ECMWF ERA5 reanalysis products have demonstrated significant improvements in Arctic and Antarctic regions, specifically for the atmospheric river events (Gorodetskaya et al., 2020a; Wille et al., 2021). Since these products provide input data for atmospheric modelling, it is important to assess limitations and errors in how well these products represent the total amount, intensity, and type of precipitation in Antarctica.

This study aims to investigate the temporal and spatial evolution of precipitation, including intensity, phase transitions, and associated temperature profiles during one week in austral summer (December 2018), when a series of extra-tropical cyclones affected the AP. To this end, we use regular measurements and measurements made as part of the Year of Polar Prediction in the Southern Hemisphere Special Observing Period (YOPP-SH SOP, Bromwich et al., 2020) from two research stations located in the western and northern AP: the Ukrainian Antarctic Akademik Vernadsky station (hereinafter Vernadsky) and the Chilean station Professor Julio Escudero (hereinafter Escudero). These are compared to ERA5 reanalysis and Polar-Weather Research and Forecasting Model (Polar-WRF) results.

## 2 Data and methods

We use ground-based meteorological observations (consisting of routine SYNOP reports) conducted during the YOPP-SH SOP in summer 2018/2019 over the Antarctic Peninsula region. Meteorological variables are compared to outputs from ERA-5 reanalysis data (Hersbach et al., 2020) and the Polar-WRF model (version 4.1.5). Polar-WRF is optimized for polar regions (Skamarock et al., 2019), including a modified land-surface model that allows variable sea-ice thickness and snow depth over sea ice to be specified (Hines & Bromwich, 2008; Bromwich et al., 2009; Hines et al., 2011).

We focus on two sites representing different regional and microclimates around the Antarctic Peninsula. One is Escudero station, situated on King George Island at the northern tip of the Peninsula (62.20°S, 58.96°W). The other is Vernadsky station — located on Galindez Island at the western, mostly upwind side closer to the central part of the Peninsula (65.25°S, 64.26°W) (see Fig. 1 for station locations). Although both stations have a maritime climate, Vernadsky is more affected by the orographic enhancement of precipitation and cold air advection from the continent (Pishniak & Beznoshchenko, 2020).

Station meteorological observations used in this study are obtained from 3-hourly SYNOP reports (World Meteorological Organization format FM12-VII for land stations). At Vernadsky, precipitation amount at the surface is measured with Tretyakov rain gauge every 24 hours. Precipitation type is determined visually every three hours. Near-surface air temperature is measured using automatic weather station thermometers (http://dskiev.com.ua/oborudovanie_troposfera.html) every 5 minutes (3-hourly data from SYNOP report are used in this study).

Meteorological and precipitation data for Escudero are obtained from 3-hourly SYNOP/METAR reports at the Base Presidente Eduardo Frei Montalva located a few hundred meters from Escudero (hereafter, we refer to measurements at both Escudero Station and Frei as Escudero). The reports include near-surface air temperature and pressure and precipitation rate and type at the time of observation (https://climatologia.meteochile.gob.cl; Carrasco & Cordero, 2020). SYNOP reports at Escudero and Vernadsky include the following types of precipitation: drizzle, rain, rain-shower, snow, snow-shower, and mix of rain and snow, as well as precipitation intensity. Snowfall intensity at Escudero is derived from snow depth measurements made every 6 hours using a ruler (with a conversion of 1 cm of snow to 1 mm of water equivalent), assuming zero precipitation for <0.5 cm snow depth and approximating snow depth of 0.6—0.9 cm to 1 cm (Carrasco & Cordero, 2020). The snowfall data were used in this study without any correction or adjustment for drifting/blowing snow deposition or removal. Also, these values are available only for snowfall, without distinguishing mixed-phase precipitation. For rainfall, only the occurrence is available (measurements of intensity and amount are lacking). Additionally, precipitation-type observations and radiosonde launches were performed at Escudero during the YOPP-SH SOP period as part of the project Characterization of the Antarctic Atmosphere and Low Clouds (Rowe et al., 2018; Gorodetskaya et al., 2020b; Bromwich et al., 2020).

The meteorological measurements are used to evaluate ERA-5 reanalysis (Hersbach et al., 2020) data, which are then used for large-scale analysis of the synoptic situation and precipitation rate and type. We use ERA5 reanalysis data for 2-m temperature, sea level pressure, total precipitation, and precipitation type, with a resolution of 0.25° × 0.25°. ERA5 precipitation records include rain, freezing rain, snow, wet snow, mixed rain and snow, and ice pellets. These data were verified against meteorological observations at both stations, with the caveat that applying SYNOP data for ERA-5 verification has some limitations due to 3-hour observed data resolution.

ERA5 provides initial and lateral boundary conditions at hourly intervals, including surface fields (dew point temperature, temperature, land-sea mask, mean sea level pressure, sea ice cover, sea surface temperature, skin temperature, snow depth, soil temperature) and pressure level fields (wind components, air temperature, geopotential height, specific and relative humidity). The Polar-WRF version 4.1.5 simulation (non-nudged) was run over a domain of 130 × 100 grid points with a spatial resolution of 9 km centered on 63°S 65°W (Fig. 1). Domain was configured in the

Lambert conformal map projection with the standard longitude of 64.0 W and true latitudes 65.0 S, and 60.0 S. Vertical resolution is 38 layers with Eta vertical coordinate type. For model relief, the ASTER GDEM v.3 topography dataset was used with a spatial resolution of 1 arc second (approximately 30-meter horizontal posting at the equator) (Abrams et al., 2020; NASA/METI/AIST/Japan Spacesystems and U.S./Japan ASTER Science Team, 2019).

The Thompson cloud microphysical parameterization scheme (Thompson et al., 2008) was chosen for the Polar-WRF simulation because of its improved representation of the Antarctic clouds (Listowski & Lachlan-Cope, 2017; Hines et al., 2019). The Thompson parameterization is a single-moment scheme with double-moment cloud ice variables (Thompson et al., 2008). In this parameterization, it is assumed that snow size distribution depends on ice water content and temperature, and snow particle shape is non-spherical with a bulk density varying inversely with diameter. Other physical parameterizations that we used in our Polar-WRF simulation are listed in Table 1.

Polar-WRF outputs used in this study include total precipitation and snow fraction of precipitation. The output is available at 30-min temporal resolution. For comparison to ERA-5 outputs, the hourly rate of total precipitation and snowfall fraction were determined.

## 3 Results

We performed a single run of Polar-WRF from 30 November (12 UTC) to 8 December 2018 (12 UTC). Our analysis focuses on 1–7 December 2018, when several periods with PPTs were observed, and there were significant precipitation amounts (Table 2) at Vernad-

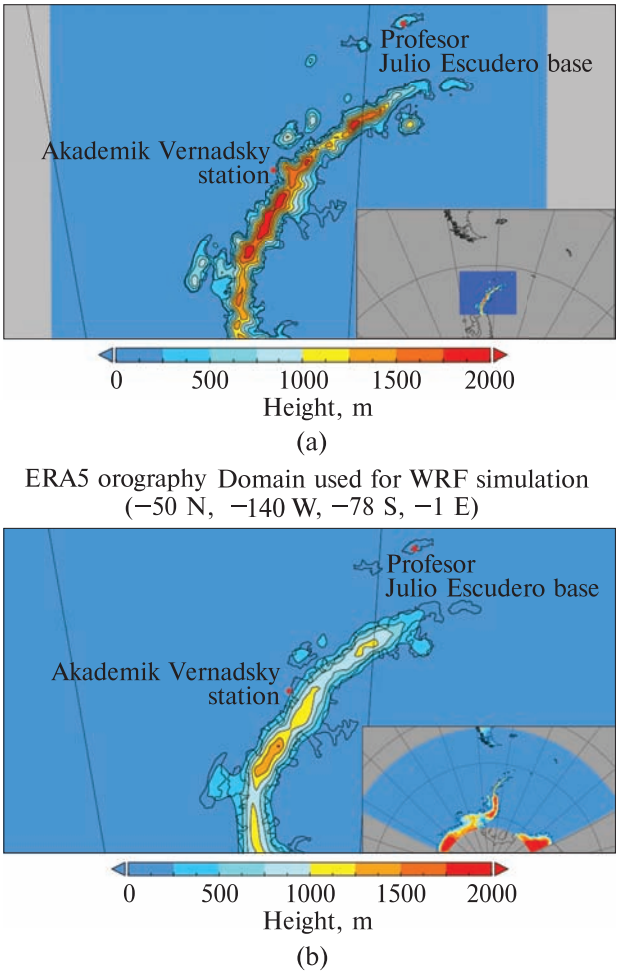


**Figure 1.** Model domain and terrain height for the Polar-WRF simulation: 130 × 100 grid points, 9 km spatial resolution, centered on 63°S 65°W (a), and in ERA5 reanalysis 0.25° × 0.25° spatial resolution, −50 N, −140 W, −78 S, −1 E domains (b). ERA5 data are used as initial and boundary conditions at the Polar-WRF domain. Red dots show the locations of Vernadsky (65.25° S, 64.26° W) and Escudero (62.20° S, 58.96° W) stations

**Table 1.** Physics parameterization schemes used in Polar-WRF simulation

| Physics options | Parameterization schemes |
|---|---|
| Micro Physics Option | Thompson Scheme (Thompson et al., 2008) |
| Cumulus parameterization | RH-dependent additional perturbation for the Kain-Fritsch scheme (Kain, 2004) |
| Shortwave radiation | Dudhia Shortwave Scheme (Dudhia, 1989) |
| Longwave radiation | RRTM Longwave Scheme (Mlawer et al., 1997) |
| Land Surface Options | Unified Noah Land Surface Model (Tewari et al., 2004) |
| Surface Layer Options | Eta Similarity Scheme (Janjić, 2002) |
| Planetary Boundary Layer | Mellor–Yamada–Janjic Scheme (MYJ) (Janjić, 1994) |

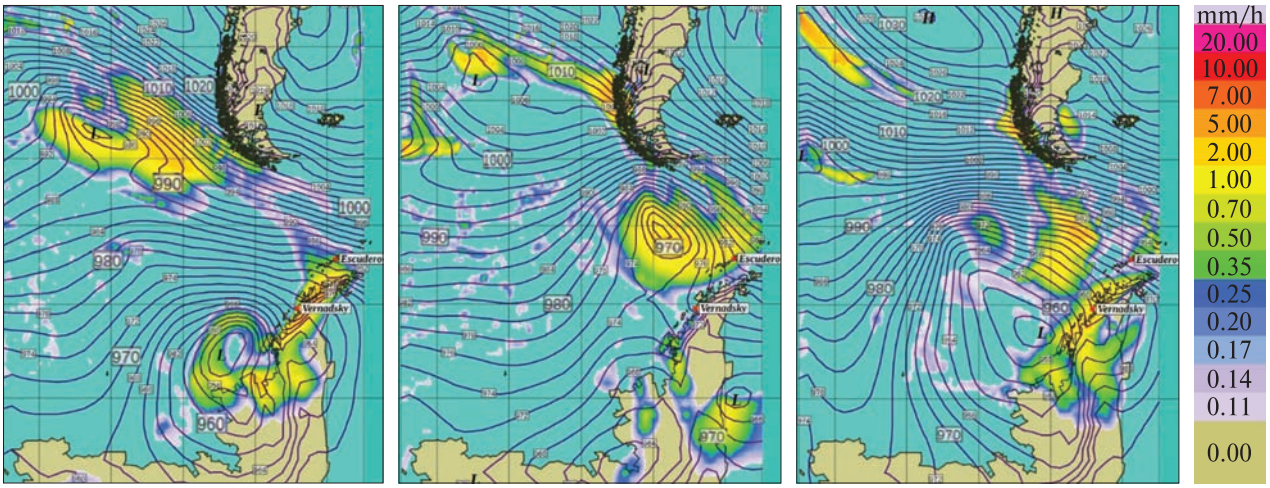


**Figure 2.** ERA5 precipitation (mm/h, colours) and mean sea level pressure (hPa, contours) at the times of precipitation phase transitions at Escudero and Vernadsky stations (plots are made in zyGrib file viewer https://www.zygrib.org)

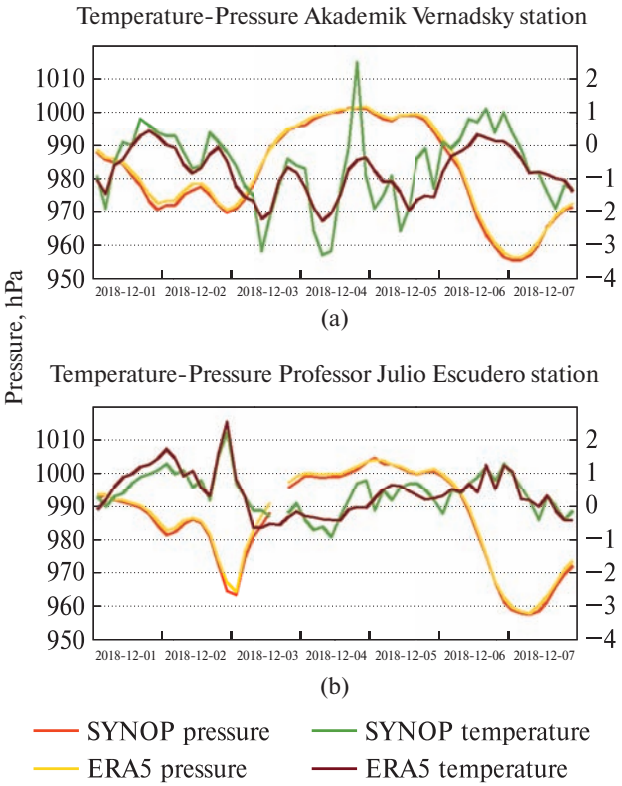


**Figure 3.** Near-surface air temperature and pressure for Vernadsky (a) and Escudero (b) stations according to measurements (SYNOP reports) and ERA5 reanalysis during 1—7 December 2018 at 3-hour temporal resolution

sky and Escudero. This period was chosen because an atmospheric river impacted AP region, and additional radiosonde observations were conducted as part of YOPP projects (Gorodetskaya et al., 2020b; Bromwich et al., 2020). Figure 2 shows mean sea level pressure and hourly precipitation spatial distributions based on ERA5 reanalysis during PPT events and/or rain occurrence at one or both stations. Three different transient synoptic-scale low-pressure systems (extratropical cyclones) passed near the western and northern AP during the first week of December (Fig. 2), each associated with near-surface pressure decrease and temperature increase at both Vernadsky and Escudero (Table 2, Fig. 3).

The first two cyclones passed near the AP within 24 hours during 1—2 December 2018, affecting both stations (Figs. 2 and 3). Table 2 shows the minimum mean sea level pressure associated with the three cyclones (bold font) from the SYNOP observations. For the first two cyclones, pressure minima occur 3 hours earlier at Vernadsky than Escudero. In between the first two cyclones, the pressure increased slightly. SYNOP data reported that for Vernadsky, near-surface pressure dropped twice to about 970 hPa associated with the passage of these cyclones — on 1 and 2 December (both at 21 UTC), with a transient in-

crease in between up to 978.6 hPa at about 12 UTC on 2 December. At Escudero, near-surface pressure dropped to 981.5 hPa (00 UTC 2December) and 963.6 hPa (00 UTC 3December), respectively, during the first and second cyclone passage. Both pressure minima occurred 3 hours later than at Vernadsky. A short pressure increase (up to 986.3 hPa) occurred 9 hours later at 9 UTC on 2 December. The third pressure minimum occurred on 7 December 2018, at 3 UTC at both stations, and reached 955.3 hPa at Vernadsky station and 957.8 hPa at Escudero.

All three cyclones were accompanied by near-surface air temperature increases at both stations that preceded the pressure minima associated with the warm front passage (Fig. 3). The time difference was greatest for the third cyclone (6–7 December): warming occurred 12 hours before the pressure minimum at Vernadsky and 9 hours in advance at Escudero. The near-surface temperature and pressure from ERA-5 are in good agreement with SYNOP data (Fig. 3). Although temperature extremes are smoothed in the ERA-5 results, the 3-hour temporal resolution captures the daily temperature change tendency (Fig. 3). When averaged over the entire week, at Escudero, the weekly mean 2-m temperature is 0.06 °C in Polar-WRF and 0.41 °C in ERA5, and at Vernadsky, it is –1.47 °C in Polar-WRF and –0.80 °C in ERA5. Thus, Polar-WRF shows, on average lower near-surface air temperature at both stations during this week in summer.

Observation data from Vernadsky and Escudero show that there was increased precipitation at both stations associated with the warm fronts of the cyclones (Table 3, Fig. 4a, 5a). According to the Polar-WRF simulations, the highes precipitation intensity at Vernadsky occurred during the low-pressure systems on 1 December and 5–6 December. At Escudero, all three low-pressure systems brought in-

**Table 2.** Timing and magnitude of the observed minimum sea level pressure (bold font) at Vernadsky and Escudero stations during cyclone passage. The short-term increase in pressure between Cyclones 1 and 2 is also shown (regular font)

| № of event | Date | Akademik Vernadsky station | | Escudero station | |
|---|---|---|---|---|---|
| | | Time (UTC) | P (hPa) | Time (UTC) | P (hPa) |
| Cyclone 1 | 2018-12-01 | 21 | **970.0** | 24 | **981.5** |
| | 2018-12-02 | 12 | 978.6 | 09 | 986.3 |
| Cyclone 2 | 2018-12-02 | 21 | **970.0** | 24 | **963.6** |
| Cyclone 3 | 2018-12-07 | 03 | **955.3** | 03 | **957.8** |

**Table 3.** Daily total precipitation amount (mm/day) over Vernadsky and Escudero stations from observations, ERA5 reanalysis, and Polar-WRF model simulation for the studied week 1–7 December 2018

| Date | Escudero station | | | Akademik Vernadsky station | | |
|---|---|---|---|---|---|---|
| | SYNOP | ERA5 | Polar-WRF | SYNOP | ERA5 | Polar-WRF |
| 2018-12-01 | 1.0 | 2.2 | 20.3 | 2.1 | 24.0 | 26.4 |
| 2018-12-02 | 2.0 | 10.2 | 20.8 | 2.4 | 3.8 | 3.1 |
| 2018-12-03 | 0.0 | 2.1 | 2.2 | 0.5 | 4.2 | 2.8 |
| 2018-12-04 | 0.0 | 0.4 | 0.5 | 0.3 | 4.2 | 3.6 |
| 2018-12-05 | 0.0 | 0.5 | 4.7 | 0.6 | 6.2 | 9.8 |
| 2018-12-06 | 8.0 | 10.8 | 27.6 | 1.5 | 31.7 | 27.9 |
| 2018-12-07 | 2.0 | 3.5 | 1.3 | 5.7 | 7.8 | 4.8 |

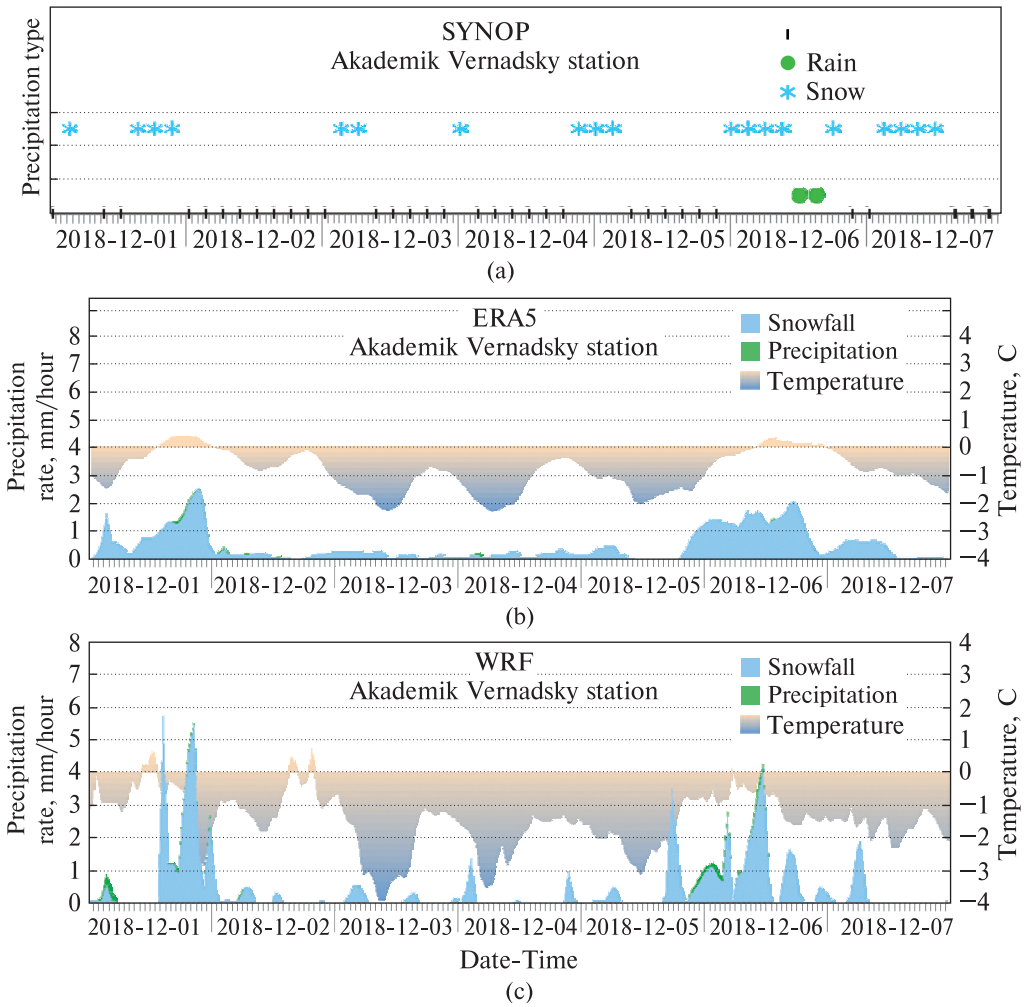


**Figure 4.** Precipitation type and rate at Vernadsky station: (a) SYNOP 3-hourly precipitation type (blue asterisks — snowfall, green circles — rain, black lines — no precipitation at the reported term; (b) ERA5 and (c) Polar-WRF hourly precipitation rate by type (bottom, green — total precipitation, blue — snowfall) and 2-m air temperature (top, scaled colour)

creased precipitation — on 1, 2, and 5–6 December (Figs. 4c and 5c). It is important to note that at Escudero, the observations likely do not correctly capture rainfall, as precipitation measurements were determined from snow height measurements assuming constant density. A possible reason for higher precipitation amounts in Polar-WRF is that Polar-WRF can better capture the orography of Escudero than ERA5, given that Escudero is situated on a small island. For Vernadsky, SYNOP shows much less precipitation sums as well, but it is due to the well-known deficiency of the Tretyakov rain gauge to measure snowfalls (Table 3).

Snowfall was observed at Vernadsky during all days except for 2 December, and rainfall was observed only on 6 December (Fig. 4a). ERA5 and Polar-WRF show a general agreement of snowfall events' occurrence and a small amount of rain on 6 December (Fig. 4). At Escudero, observations show a predominance of rain and rain-snow mixture during all three cyclone passages on 1–2 and 6–7 December (Fig. 5a). This phase transition at Escudero is different in ERA5 and

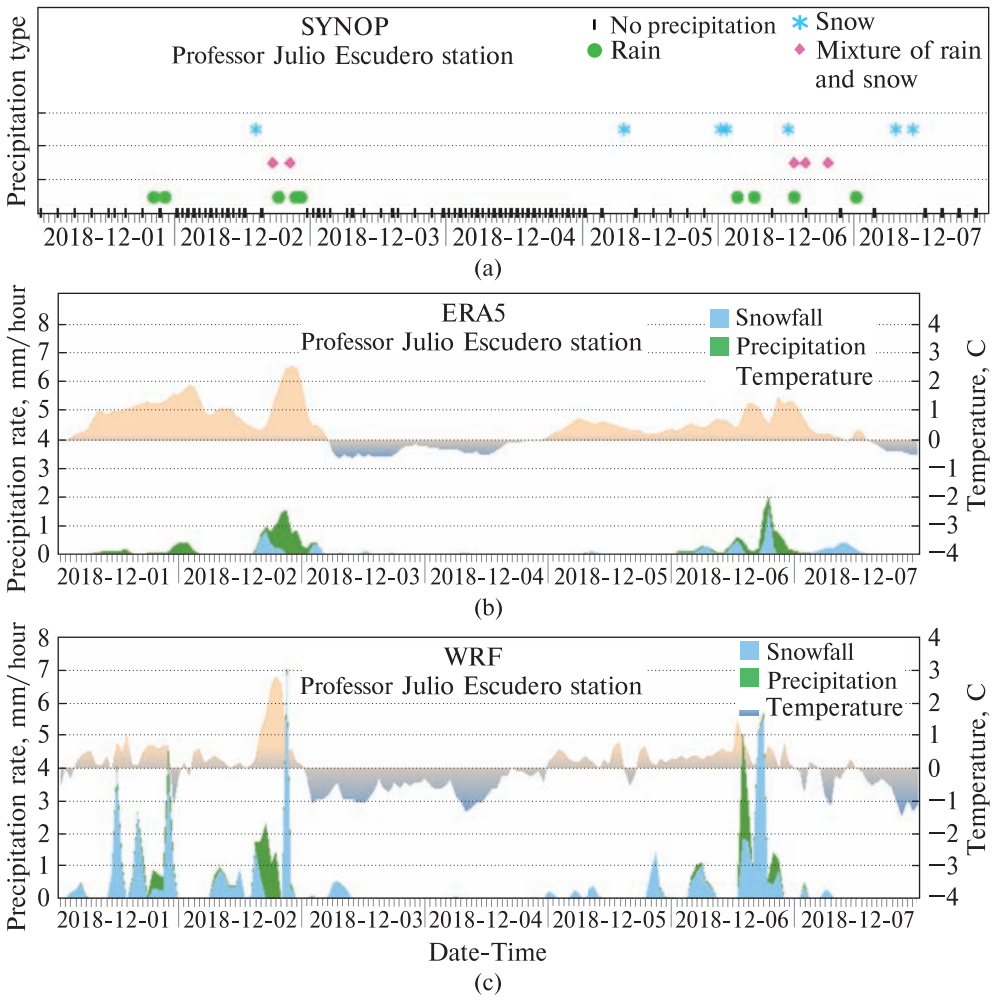


**Figure 5.** Precipitation type and rate at Escudero station: (a) SYNOP 3-hourly precipitation type (blue asterisks — snowfall, green circles — rain, black lines — no precipitation at the reported term; (b) ERA5 and (c) Polar-WRF hourly precipitation rate by type (bottom, green — total precipitation, blue — snowfall) and 2-m air temperature (top, scaled colour)

Polar-WRF (Fig. 5). Below we discuss in detail precipitation intensities and phase transition, together with temperature dependence for each event.

At Escudero, PPT from snow to rain and lower pressure minimum were observed later than over Vernadsky from 21 UTC 2 December to 00 UTC 3 December. This event was associated with a passage of another extra-tropical cyclone (Fig. 2, center). It should be mentioned that the lowest pressure observed during December 6 and 7 corresponds to the same pressure low with PPT between rain and snow and/or mixed-phase precipitation for both stations (Figs. 2, 3, 4a, 5a).

Polar-WRF simulated higher precipitation rates (of a more intermittent character) compared to ERA5 both at Vernadsky and Escudero, especially during the three low-pressure system passages (Table 2, Figs. 4 and 5). During the entire week, ERA5 shows a predominance of snow in total precipitation at Vernadsky (Fig. 4b), even when near-surface air temperature increased above 0 °C on the 1st and 6th of December. This could indicate a mixture of rain and snow or wet

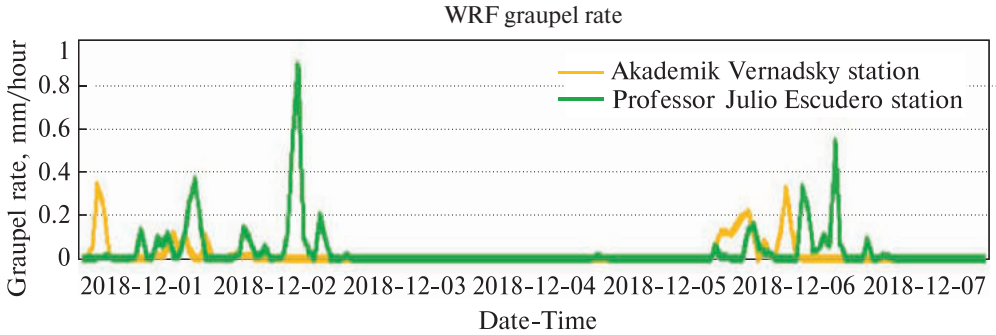


**Figure 6.** Polar-WRF graupel fraction rate of total hourly precipitation (mm/hour). The green line marks Escudero station, yellow line —Vernadsky station

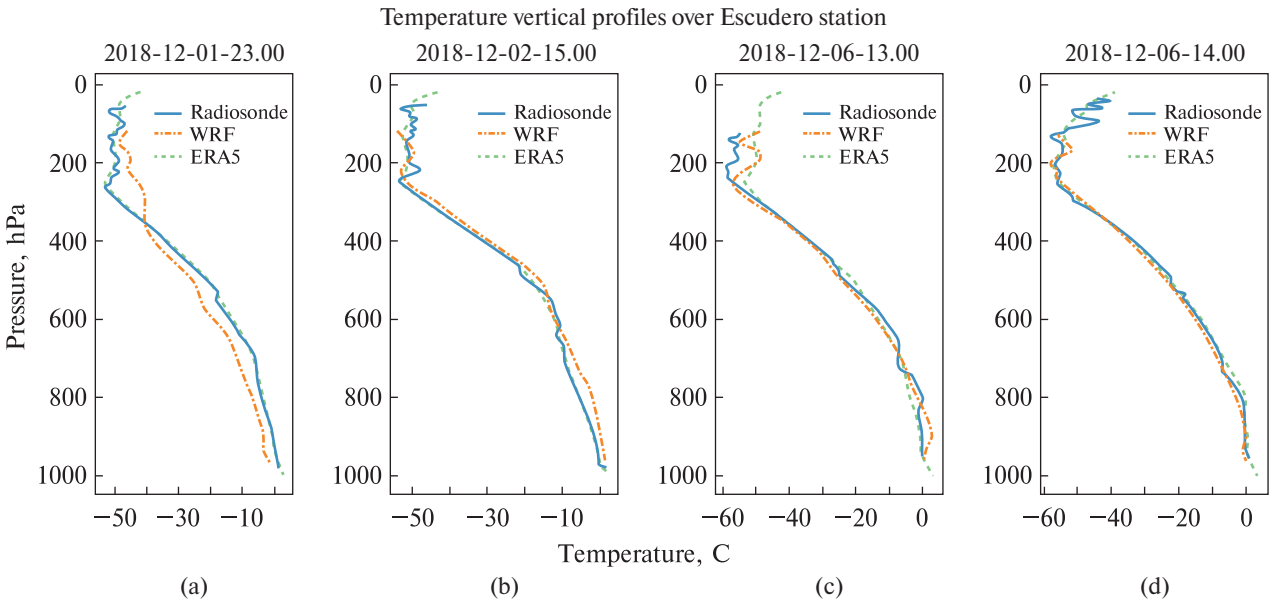


**Figure 7.** Air temperature vertical profiles over Escudero station: from radiosonde measurements (solid blue line), and derived for the closest grid for ERA5 reanalysis (dashed green line), and Polar-WRF (dashed orange line)

snow. Polar-WRF simulation shows lower temperatures and a more intermittent distribution of precipitation during the week with higher intensities than the more smoothed ERA5 precipitation distribution at both stations. For Vernadsky, Polar-WRF forecasts snowfall and temperatures below 0 °C predominantly. However, there are indications of rain during December 1 and 6 (green dots in Fig. 4a); based on the temperature, the rain was most likely supercooled.

Higher amounts of rain are found at Escudero compared to Vernadsky (Figs. 4, 5) according to both ERA5 and Polar-WRF precipitation rate data, in concordance with the predominance of temperatures above 0 °C observed and simulated by the models at Escudero during the studied period (Figs. 3 and 5b, c).

Polar-WRF simulated results indicate graupel (up to 0.9 mm/h) at both stations during 1, 2, and 6 December (Fig. 6). The highest graupel precipitation rate corresponds to pressure lows, increased precipitation rate, and a mixture of rain and snow.

Figure 7 shows vertical temperature profiles at Escudero during the times with PPT events using radiosonde measurements conducted during the YOPP-SH SOP. These measurements are used to evaluate the

ERA5 and Polar-WRF products at the grid points corresponding to the station location. ERA5 represents vertical profiles well. Polar-WRF shows lower temperatures in the lower troposphere during the first event on 1 December compared to radiosonde and ERA5, while other Polar-WRF profiles are much closer to radiosonde data. Lower temperatures in the first profile could explain the larger snow fraction in the total precipitation in Polar-WRF simulated results for the first event compared to ERA5 data. Thus, ERA5 represents temperature profile and precipitation better than Polar-WRF downscaling for the event on 1 December.

For the event on 2 December, there is a good correspondence in vertical temperature profile between radiosonde measurements and ERA5, while Polar-WRF shows a significant positive bias (Fig. 7b). At the same time, both ERA5 and Polar-WRF simulation represent well the occurrence of the mixed-phase precipitation (rain and snow) and PPT at Escudero during this event (Fig. 5). However, Polar-WRF still simulates a much higher snowfall rate compared to ERA5.

Different temperature and precipitation characteristics were observed and simulated for the event on 6 December. Gorodetskaya et al. (2020b) and Bromwich et al. (2020) showed that this event was associated with an atmospheric river, affecting both southern South America and the Antarctic Peninsula. Radiosonde measurements at Escudero on 6 December 2018, 13 UTC, demonstrated a temperature inversion at around 800 hPa exceeding 0 °C at the inversion height and in the layer between it and the surface (Fig. 7). At the exact time, temperature inversion was represented by the Polar-WRF but at lower heights, while ERA5 reanalysis missed it. Thus, unlike other events discussed above, Polar-WRF temperature representation is more accurate than ERA5. As during earlier events, Polar-WRF simulated higher precipitation rates compared to ERA5 both at Escudero and Vernadsky stations (Figs. 4 and 5) and compared to observations (Table 1). At the same time, Polar-WRF shows a good correspondence of the timing of rain occurrence compared to observations, while ERA5 misses some rain occurrence and shows more preference for snowfall. This more realistic representation of precipitation phase (rainfall occurrence) simulated by Polar-WRF during 6 December compared to ERA5 can be related to the improved temperature representation in the model.

## 4 Discussion and conclusions

This study analysed three different transient synoptic-scale low-pressure systems (extra-tropical cyclones) passing near the western and northern AP during the first week of December 2018. The cases and associated evolution of temperature and precipitation (amount and phase transitions) were analysed using observations at Vernadsky (65.25°S, 64.26°W) and Escudero (62.20°S, 58.96°W), ERA5 reanalysis (30-km spatial resolution) and Polar-WRF simulations at 9-km spatial resolution. For the Polar-WRF model simulation forced by ERA5, we used Thompson et al. (2008) cloud/precipitation microphysics parameterization. This parameterization showed a good combination of relatively low required computational resources and a satisfactory representation of the precipitation phase and the timings of precipitation phase transition.

Each cyclone passage was associated with near-surface pressure decrease and temperature increase at both Vernadsky and Escudero. ERA5 and Polar-WRF overestimated precipitation amounts during these cyclones compared to observations at the Escudero and Vernadsky. However, it should be considered that precipitation measurements done at both stations at the studied period have biases in polar regions usually associated with high winds and blowing snow. Moreover, precipitation amount measurements at Escudero included only snowfall amounts (based on snow depth changes), while only the occurrence was reported for rainfall. To improve precipitation measurement capacity at Vernadsky, the Micro Rain Radar MRR-Pro (Metek's vertically profiling 24-GHz precipitation radar) and the Lufft WS100 radar precipitation sensor have been recently installed. With an automatic weather station already installed at the Vernadsky, these new precipitation high-precision instruments will be used for precipitation amount and type analysis and model evaluation in the future.

The Polar-WRF model forecasts 2-m air temperature averages that are low compared to ERA5 and SYNOP data during the studied week. It is important to note that results from longer-term studies in different regions of the Antarctic Peninsula suggest that Polar-WRF near-surface temperatures are biased-low with respect to observations. These studies found the cold biases associated with biased-low downward longwave radiation (Bromwich et al., 2013; King et al., 2015; Deb et al., 2016; Listowski & Lachlan-Cope, 2017; Bozkurt et al., 2020; 2021). Future studies should, therefore, compare downward radiation forecasts from Polar-WRF to measurements and explore how more sophisticated microphysics schemes might reduce biases in downward longwave radiation.

The overall lower 2-m air temperature forecasted by the Polar-WRF model, in combination with higher spatial resolution, better representation of topography, and more advanced cloud and precipitation microphysics, could explain the higher simulated amounts of total precipitation and snow fraction in comparison to ERA5 data. For each low-pressure system, different results regarding biases in each model were obtained. For the event on 1 December, the Polar-WRF shows lower temperatures than radiosonde measurements at Escudero, while the ERA5 temperature profile shows a good correspondence. On 2 December, ERA5 corresponds well to the vertical temperature profile, while Polar-WRF simulates a warmer lower troposphere than the radiosondes. While no precipitation was observed at Vernadsky, both models simulated low rates of snowfall at Vernadsky. The models simulated a mixture of snowfall and rainfall and precipitation phase transitions at Escudero station in good agreement with observations.

The low-pressure system affecting the Antarctic Peninsula during 6 December was associated with an atmospheric river event, with a significant temperature inversion in the lower troposphere apparent in the radiosounding at Escudero station. As Gorodetskaya et al. (2020b) and Bromwich et al. (2020) described, this temperature inversion layer also showed a significant moisture inversion, and a peak in the moisture flux observed at the Escudero station. This temperature inversion was not captured by the ERA5 temperature profile, while Polar-WRF data simulated it well, however, with a slight shift towards the lower heights. Also, the Polar-WRF precipitation phase better corresponds to observations compared to ERA5 reanalysis, including the timings of precipitation phase transition between rainfall, snowfall, and mixed-phase precipitation.

In addition, graupel fraction was present in the total precipitation during all events according to Polar-WRF. This further highlights the microphysical scheme used in Polar WRF (Thompson parameterization scheme) being more advanced than ERA5. The associated causes should be studied in more detail in the future.

To summarise, the ERA5 reanalysis and Polar-WRF model both demonstrated a good correspondence of precipitation phase compared to observations for the events occur over the week-long study period. Overall, Polar-WRF simulations were found to better represent detailed structure and distributions of precipitation and temperature, while such features were found to be more smoothed out in ERA5 reanalysis data. At the same time, model biases were found and, despite the additional observations made during the YOPP SOP, measurements were insufficient to understand the underlying reasons. Thus, our work shows the importance of additional measurements such as those made during the YOPP SOP. We highlight the necessity of increasing the number of radiosoundings in Antarctica and including more robust precipitation measurements to better investigate models' ability to simulate precipitation and precipitation phase transitions. Our study also demonstrated the added value of combining observations from stations located in the western and northern Antarctic Peninsula, particularly for characterizing precipitation during synoptic events affecting the entire Antarctic Peninsula.

*Author contributions.* Conceptualization — IG; WRF model setup and simulations — AC; post-processing of model output — AC and DP; measurement data processing — AC, IG, PR; analysing and discussing the results — all; writing —original draft preparation — AC, IG; writing — review and editing — IG, SK, PR.

*Acknowledgment.* Reanalysis data for this study is provided by the European Center for Medium-Range

Weather Forecasts (ECMWF) and is available via the Copernicus Climate Change Service Climate Data Store (https://cds.climate.copernicus.eu). Polar-WRF developed by the Polar Meteorology Group of the Byrd Polar Research and Climate Center at The Ohio State University (http://polarmet.osu.edu/hines/PWRF/) and WRF-ARW available from National Center for Atmospheric Research (http://www.mmm.ucar.edu/wrf/users/download/get_source.html). SYNOP observations are available via Meteomanz.com. State Institution National Antarctic Scientific Center for Akademik Vernadsky station meteorological data available at http://meteodata.uac.gov.ua.

The authors are grateful to the Chilean Antarctic Institute (INACH) for logistical support and to the Antarctic Research Group (http://antarctica.cl), Universidad de Santiago de Chile (USACH) for supporting and maintaining the research platform at Escudero Station and help with radiosonde observations. Personnel at both Frei and Akademik Vernadsky stations is thanked for providing SYNOP reports. This is a contribution to the Year of Polar Prediction (YOPP), a flagship activity of the Polar Prediction Project (PPP), initiated by the World Weather Research Programme (WWRP) of the World Meteorological Organisation (WMO).

We greatly thank the anonymous reviewers for the insightful and valuable comments and suggestions that help us to improve our paper.

*Funding.* IG thanks FCT/MCTES for the financial support to CESAM (UIDP/50017/2020+UIDB/50017/2020) and FCT project ATLACE (CIRCNA/CAC/0273/2019) through national funds.

*Conflict of Interest.* The authors declare that they have no conflict of interest.

**References**

Abrams, M., Crippen, R., & Fujisada, H. (2020). ASTER Global Digital Elevation Model (GDEM) and ASTER Global Water Body Dataset (ASTWBD). *Remote Sensing*, 12(7), 1156. https://doi.org/10.3390/rs12071156

Agosta, C., Fettweis, X., & Datta, R. (2015). Evaluation of the CMIP5 models in the aim of regional modelling of the Antarctic surface mass balance. *The Cryosphere*, 9(6), 2311–2321. https://doi.org/10.5194/tc-9-2311-2015

Bozkurt, D., Bromwich, D. H., Carrasco, J., Hines, K. M., Maureira, J. C., & Rondanelli, R. (2020). Recent near-surface temperature trends in the Antarctic Peninsula from observed, reanalysis and regional climate model data. *Advances in Atmospheric Sciences*, 37, 477–493. https://doi.org/10.1007/s00376-020-9183-x

Bozkurt, D., Bromwich, D. H., Carrasco, J., & Rondanelli, R. (2021). Temperature and precipitation projections for the Antarctic Peninsula over the next two decades: Contrasting global and regional climate model simulations. *Climate Dynamics*, 56, 3853–3874. https://doi.org/10.1007/s00382-021-05667-2

Bromwich, D.H., Hines, K.M., & Bai, L.S. (2009). Development and testing of Polar Weather Research and Forecasting model: 2. Arctic Ocean. *Journal of Geophysical Research: Atmospheres*, 114(D08), 122. https://doi.org/10.1029/2008JD010300

Bromwich, D. H., Nicolas, J. P., Hines, K. M., Kay, J. E., Key, E. L., Lazzara, M. A., Lubin, D., McFarquhar, G. M., Gorodetskaya, I. V., Grosvenor, D. P., Lachlan-Cope, T., & Van Lipzig, N. P. M. (2012). Tropospheric clouds in Antarctica. *Reviews of Geophysics*, 50 (1), (RG1004). https://doi.org/10.1029/2011RG000363

Bromwich, D. H., Otieno, F. O., Hines, K. M., Manning, K. W., & Shilo, E. (2013). Comprehensive evaluation of polar weather research and forecasting model performance in the Antarctic. *Journal of Geophysical Research: Atmospheres*, 118(2), 274–292. https://doi.org/10.1029/2012jd018139

Bromwich, D. H., Werner, K., Casati, B., Powers, J. G., Gorodetskaya, I. V., Massonnet, F., Vitale, V., Heinrich, V. J., Liggett, D., Arndt, S., Barja, B., Bazile, E., Carpentier, S., Carrasco, J. F., Choi, T., Choi, Y., Colwell, S. R., Cordero, R. R., Gervasi, M., Haiden, T., Hirasawa N., Inoue, J., Jung, T., Kalesse, H., Kim, S.-J., Lazzara, M. A., Manning, K. W., Norris, K., Park, S.-J., Reid, P., Rigor, I., Rowe, P. M., Schmithüsen, H., Seifert, P., Sun, Q., Uttal, T., Zannoni, M., & Zou, X. (2020). The Year of Polar Prediction in the Southern Hemisphere (YOPP-SH). *Bulletin of the American Meteorological Society*, 101(10), E1653-E1676. https://doi.org/https://doi.org/10.1175/BAMS-D-19-0255.1

Carrasco, J. F. & Cordero, R. R. (2020). Analyzing Precipitation Changes in the Northern Tip of the Antarctic Peninsula during the 1970–2019 Period. *Atmosphere*, 11(12), 1270. https://doi.org/10.3390/atmos11121270

Chyhareva, A., Krakovska, S., & Pishniak, D. (2019). Climate projections over the Antarctic Peninsula region to the end of the 21st century. Part II: wet/dry indices. *Ukrainian Antarctic Journal*, 2(19), 47–63. https://doi.org/10.33275/1727-7485.2(19).2019.151

Dai, A. (2008). Temperature and pressure dependence of the rain-snow phase transition over land and ocean. *Geophysical Research Letters*, 35(12), L12802. https://doi.org/10.1029/2008GL033295

Deb, P., Orr, A., Hosking, J. S., Phillips, T., Turner, J., Bannister, D., Pope, J. O., & Colwell, S. (2016). An assessment

of the Polar Weather Research and Forecasting (WRF) model representation of near-surface meteorological variables over West Antarctica. *Journal of Geophysical Research: Atmospheres*, 121(4), 1532–1548. https://doi.org/10.1002/2015jd024037

Dudhia, J. (1989). Numerical study of convection observed during the Winter Monsoon Experiment Using a Mesoscale Two–Dimensional Model. *Journal of the Atmospheric Sciences*, 46(20), 3077–3107. https://doi.org/10.1175/1520-0469(1989)046<3077:NSOCOD>2.0.CO;2

Gonzalez, S., Vasallo, F., Recio-Blitz, C., Guijarro, J. A., & Riesco, J. (2018). Atmospheric Patterns over the Antarctic Peninsula. *Journal of Climate*, 31(9), 3597—3608. https://doi.org/10.1175/JCLI-D-17-0598.1

Gorodetskaya, I. V., Silva, T., Schmithüsen, H. & Hirasawa, N. (2020a). Atmospheric River Signatures in Radiosonde Profiles and Reanalyses at the Dronning Maud Land Coast, East Antarctica. *Advances in Atmospheric Sciences,* 37, 455–476. https://doi.org/10.1007/s00376-020-9221-8

Gorodetskaya, I. V., Rowe, P. M., Kalesse, H., Silva, T., Hirasawa, N., Schmithüsen, H., Seifert, P., Park, S.-J., Choi, Y., & Cordero, R. R. (2020b). The vertical structure of atmospheric rivers and their impact in the Atlantic sector of Antarctica from the Year of Polar Prediction observations. *EGU General Assembly 2020, Online, 4–8 May 2020*, EGU2020-20313. https://doi.org/10.5194/egusphere-egu2020-20313

Hersbach, H., Bell, B., Berrisford, P., Hirahara, S., Horányi, A., Muñoz-Sabater, J., Nicolas, J., Peubey, C., Radu, R., Schepers, D., Simmons, A., Soci, C., Abdalla, S., Abellan, X., Balsamo, G., Bechtold, P., Biavati, G., Bidlot, J., Bonavita, M., De Chiara, G., Dahlgren, P., Dee, D., Diamantakis, M., Dragani, R., Flemming, J., Forbes, R., Fuentes, M., Geer, A., Haimberger, L., Healy, S., Hogan, R. J., Hólm, E., Janisková, M., Keeley, S., Laloyaux, P., Lopez, P., Lupu, C., Radnoti, G., de Rosnay, P., Rozum, I., Vamborg, F., Villaume, S., & Thépaut, J.-N. (2020). The ERA5 global reanalysis. *Quarterly Journal of the Royal Meteorological Society*, 146(730), 1999—2049. https://doi.org/10.1002/qj.3803

Hines, K. M., & Bromwich, D. H. (2008). Development and testing of Polar Weather Research and Forecasting (WRF) model. Part I: Greenland ice sheet meteorology. *Monthly Weather Review*, 136(6), 1971–1989. https://doi.org/10.1175/2007MWR2112.1

Hines, K. M., Bromwich, D. H., Bai, L.-S., Barlage, M., & Slater, A. G. (2011). Development and testing of Polar WRF. Part III: Arctic Land. *Journal of Climate*, 24(1), 26–48. https:// doi.org/10.1175/2010JCLI3460.1

Hines, K. M., Bromwich, D. H., Wang, S.-H., Silber, I., Verlinde, J., & Lubin, D. (2019). Microphysics of summer clouds in central West Antarctica simulated by the Polar Weather Research and Forecasting Model (WRF) and the Antarctic Mesoscale Prediction System (AMPS). *Atmospheric Chemistry and Physics*, 19(19), 12431–12454. https://doi.org/10.5194/acp-19-12431-2019

IMBIE team, Shepherd, A., Ivins, E., Rignot, E., Smith, B., van den Broeke, M., Velicogna, I., Whitehouse, P., Briggs, K., Joughin, I., Krinner, G., Nowicki, S., Payne, T., Scambos, T., Schlegel, N., A, G., Agosta, C., Ahlstrøm, A., Babonis, G., Barletta, V., Blazquez, A., ... Wouters, B. (2018). Mass balance of the Antarctic Ice Sheet from 1992 to 2017. *Nature*, 558(7709), 219–222. https://doi.org/10.1038/s41586-018-0179-y

Janjić, Z. I. (1994). The Step–Mountain Eta Coordinate Model: Further developments of the convection, viscous sublayer, and turbulence closure schemes. *Monthly Weather Review*, 122(5), 927–945. https://doi.org/10.1175/1520-0493-(1994)122<0927:TSMECM>2.0.CO;2

Janjić, Z. I. (2002). Nonsingular implementation of the Mellor-Yamada Level 2.5 Scheme in the NCEP Meso model. *NCEP Office Note No*. 437, 61 pp.

Jones, M. E., Bromwich, D. H., Nicolas, J. P., Carrasco, J., Plavcová, E., Zou, X., & Wang, A. S.-H. (2019). Sixty Years of Widespread Warming in the Southern Middle and High Latitudes (1957—2016). *Journal of Climate*, 32(20), 6875–6898. https://doi.org/10.1175/JCLI-D-18-0565.1

Kain, J. S. (2004). The Kain–Fritsch convective parameterization: An update. *Journal of Applied Meteorology and Climatology*, 43(1), 170–181. https://doi.org/10.1175/1520-0450(2004)043<0170:TKCPAU>2.0.CO;2

Kay, J. E., Bourdages, L., Miller, N. B., Morrison, A., Yettella, V., Chepfer, H., & Eaton, B. (2016). Evaluating and improving cloud phase in the Community Atmosphere Model version 5 using spaceborne lidar observations. *Journal of Geophysical Research: Atmospheres*, 121(8), 4162–4176. https://doi.org/10.1002/2015JD024699

King, J. C., Gadian, A., Kirchgaessner, A., Kuipers Munneke, P., Lachlan-Cope, T. A., Orr, A., Reijmer, C., van den Broeke, M. R., van Wessem, J. M., & Weeks, M. (2015). Validation of the summertime surface energy budget of Larsen C Ice Shelf (Antarctica) as represented in three high-resolution atmospheric models. *Journal of Geophysical Research: Atmospheres*, 120(4), 1335—1347. https://doi.org/10.1002/2014JD022604.

Krakovskaia, S. V., & Pirnach, A. M. (2000). Theoretical study formation and development of antarctic cloudiness under different intensity of ice and cloud droplet nucleation. *AIP Conference Proceedings*, 534 (1), 467. https://doi.org/10.1063/1.1361908

Krakovskaia, S., & Pirnach, A. (2003). Mesoscale and Microphysical Features of Frontal Rainbands in the Deep Depression of Explosive Cyclone Type over the Antarctic Peninsula. *Ukrainian Antarctic Journal*, 1, 85—92. https://doi.org/10.33275/1727-7485.1.2003.629

Lachlan-Cope, T., Listowski, C., & O'Shea, S. (2016). The microphysics of clouds over the Antarctic Peninsula – Part 1: Observations. *Atmospheric Chemistry and Physics*, 16 (24), 15605–15617. https://doi.org/10.5194/acp-16-15605-2016

Listowski, C., & Lachlan-Cope, T. (2017). The microphysics of clouds over the Antarctic Peninsula — Part 2: modelling aspects within Polar-WRF. *Atmospheric Chemistry and Physics*, 17(17), 10195–10221. https://doi.org/10.5194/acp-17-10195-2017

Mlawer, E. J., Taubman, S. J., Brown, P. D., Iacono, M. J., & Clough, S. A. (1997). Radiative transfer for inhomogeneous atmospheres: RRTM, a validated correlated–k model for the longwave. *Journal of Geophysical Research: Atmospheres*, 102 (D14), 16663–16682. https://doi.org/10.1029/97JD00237

NASA/METI/AIST/Japan Spacesystems and U.S./Japan ASTER Science Team (2019). *ASTER Global Digital Elevation Model V003* [Data set]. NASA EOSDIS Land Processes DAAC. https://doi.org/10.5067/ASTER/ASTGTM.003

Nicolas, J. P., Vogelmann, A. M., Scott, R. C., Wilson, A. B., Cadeddu, M. P., Bromwich, D. H., Verlinde, J., Lubin, D., Russell, L. M., Jenkinson, C., Powers, H. H., Ryczek, M., Stone, G., & Wille, J. D. (2017). January 2016 extensive summer melt in West Antarctica favoured by strong El Niño. *Nature Communications*, 8, 15799. https://doi.org/10.1038/ncomms15799

Pishniak, D., & Beznoshchenko, B. (2020). Improving the detailing of atmospheric processes modelling using the Polar WRF model: a case study of a heavy rainfall event at the Akademik Vernadsky station. *Ukrainian Antarctic Journal*, 2, 26—41. https://doi.org/10.33275/1727-7485.2.2020.650

Rignot, E., Mouginot, J., Scheuchl, B., van den Broeke, M., van Wessem, M. J., & Morlighem, M. (2019). Four decades of Antarctic Ice Sheet mass balance from 1979–2017. *Proceedings of the National Academy of Sciences of the USA*, 116(4), 1095—1103. https://doi.org/10.1073/pnas.1812883116

Rowe, P. M, Sepulveda, E., Neshyba, S. P., Caballero, M., Damiani, A., & Cordero, R. (2018). The radiative impact of clouds over the Antarctic Peninsula and Southern Ocean. *15th Conference on Cloud Physics/Atmospheric Radiation, 9–13 July 2018, Vancouver, BC*. Retrieved September 20, 2020, from https://ams.confex.com/ams/15CLOUD15ATRAD/webprogram/Paper347761.html

Skamarock, W. C., Klemp, J. B., Dudhia, J., Gill, D. O., Liu, Z., Berner, J., Wang, W., Powers, J. G., Duda, M. G., Barker, D., & Huang, X.-Y. (2019). *A Description of the Advanced Research WRF Model Version 4* (No, NCAR/TN-556+STR), 145. https://doi.org/10.5065/1dfh-6p97

Tewari, M., Chen, F., Wang, W., Dudhia, J., Le Mone, M. A., Mitchell, K., Ek, M., Gayno, G., Wegiel, J., & Cuenca, R. H. (2004). Implementation and verification of the unified NOAH land surface model in the WRF model. *20th Conference on Weather Analysis and Forecasting/16th Conference on Numerical Weather Prediction*, 14.2A. Retrieved September 20, 2020, from https://ams.confex.com/ams/84Annual/techprogram/paper_69061.htm

Thompson, G., Field, P. R., Rasmussen, R. M., & Hall, W. D. (2008). Explicit Forecasts of Winter Precipitation Using an Improved Bulk Microphysics Scheme. Part II: Implementation of a New Snow Parameterization. *Monthly Weather Review*, 136(12), 5095–5115. https://doi.org/10.1175/2008MWR2387.1

Turner, J., Lachlan-Cope, T., Thomas, J. P., & Colwell, S. R. (1995). The synoptic origins of precipitation over the Antarctic Peninsula. *Antarctic Science*, 7(3), 327—337. https://doi.org/10.1017/S0954102095000447

Vignon, É., Roussel, M.-L., Gorodetskaya, I. V., Genthon, C., & Berne, A. (2021). Present and Future of Rainfall in Antarctica. *Geophysical Research Letters,* 48(8), e2020GL092281. https://doi.org/10.1029/2020GL092281

Wille, J. D., Favier, V., Dufour, A., Gorodetskaya, I. V., Turner, J., Agosta, C., & Codron, F. (2019). West Antarctic surface melt triggered by atmospheric rivers. *Nature Geoscience*, 12(11), 911–916. https://doi.org/10.1038/s41561-019-0460-1

Wille, J. D., Favier, V., Gorodetskaya, I. V., Agosta, C., Kittel, C., Beeman, J. C., Jourdain, N. C., Lenaerts, J. T. M., & Codron, F. (2021). Antarctic atmospheric river climatology and precipitation impacts. *Journal of Geophysical Research: Atmospheres*, 126(8), e2020JD033788. https://doi.org/10.1029/2020JD033788

Yuter, S. E., Kingsmill, D. E., Nance, L. B., & Löffler-Mang, M. (2006). Observations of Precipitation Size and Fall Speed Characteristics within Coexisting Rain and Wet Snow. *Journal of Applied Meteorology and Climatology*, 45(10), 1450–1464. https://doi.org/10.1175/JAM2406.1

Received: 6 April 2021
Accepted: 14 June 2021

**А. Чигарева [1, 2, *], І. Городецька [3], С. Краковська [1, 2, *], Д. Пішняк [2], П. Ров [4]**

[1] Український гідрометеорологічний інститут ДСНС України та НАН України, м. Київ, 03028, Україна
[2] Державна установа Національний антарктичний науковий центр МОН України, м. Київ, 01601, Україна
[3] Центр екологічних та морських досліджень, фізичний факультет, Університет Авейру, м. Авейру, 3810-193, Португалія
[4] Північно-західна дослідницька асоціація Редмонд, штат Вашингтон, 98052, США

*** Автори для кореспонденції:** chyhareva@ukr.net, svitlanakrakovska@gmail.com

**Зміна фазового стану опадів під час південнополярного літа в районі Антарктичного півострова**

**Абстракт.** Зміни фазового стану опадів мають вирішальне значення для розуміння процесів формування та впливу опадів, особливо в полярних регіонах. У цьому дослідженні використовуються дані спостережень та чисельні моделі для дослідження зміни фази опадів на захід та на північ від Антарктичного півострова впродовж південнополярного літа. Дослідження проведено на основі даних реаналізу ERA5 та результатах обчислень моделі Polar-WRF (The Weather Research and Forecasting), що були порівняні з даними регулярних метеорологічних спостережень та додаткових вимірювань, проведених під час спеціального періоду спостережень у рік полярного прогнозування (Year of polar prediction special observing period, YOPP-SOP). Проаналізовано три випадки проходження позатропічних циклонів, під час яких були зафіксовані опади зі зміною фазового стану, над чилійською станцією «Професор Хуліо Ескудеро» (острів Кінг Джордж, на північ від Антарктичного півострова) та над Українською антарктичною станцією «Академік Вернадський» (західна сторона Антарктичного півострова) під час першого тижня грудня 2018 року. Було проаналізовано дані спостереження та моделювання приземних температури та тиску повітря, кількості та типу опадів, вертикальні профілі температури повітря. Отримані результати показують, що тип опадів (сніг чи дощ) добре представлений у моделях ERA5 та Polar-WRF, але загальна кількість опадів завищена порівняно з даними спостережень. ERA5 добре відображає добову мінливість і вертикальний профіль температури повітря, тоді як Polar-WRF занижує температуру в нижній частині тропосфери. Однак ERA5 згладжує інверсію температури під час проходження атмосферної річки, тоді як Polar-WRF цю інверсію відображає. Усереднена за тиждень температура, розрахована за допомогою Polar-WRF, нижча за ERA5. Також порівняно з ERA5 у Polar-WRF змодельована більша частка снігу в загальній кількості опадів і фазовий перехід опадів представлено краще під час події, пов'язаною з проходженням атмосферної річки. В результаті дослідження було проілюстровано взаємозв'язок між певними синоптичними умовами та фазовими переходами опадів в районі Антарктичного півострова та оцінено здатність сучасних даних реаналізу та регіональної моделі атмосфери відтворювати ці процеси.

**Ключові слова:** Антарктичний півострів, Українська антарктична станція «Академік Вернадський», чилійська станція «Професор Хуліо Ескудеро», фаза опадів, ERA5, Polar-WRF, температура повітря, атмосферний тиск